International Journal of Academic Engineering Research (IJAER)
ISSN: 2000-001X
Vol. 3 Issue 2, February – 2019, Pages: 1-14

Analytical Modelling, Simulation and Implementation of Solar Tracker

A. A. M. Hassan[(1)] ali_eltallawy@yahoo.com
Adel A. Elbaset[(2)] Adel.Soliman@mu.edu.eg
A. T. Hasouna[(3)] AT_hasoune@hotmail.com
Amr Emad[(3)] Engamremad77@yahoo.com

[(1)]*Department of Power Engineering and Energy , Faculty of Engineering ,Minia university, El-Minia, 61517, Egypt*
[(2)]*Electrical Engineering Department, Faculty of Engineering ,Minia university, El-Minia, 61517, Egypt*
[(3)]*Dept. of Mechanical Eng., El-Minia High Institute for Engineering and Technology, El-Minia, Egypt*

Abstract *- The aim of this work is to develop a microcontroll er-based solar tracking system and assess the value of using single and dual-axis solar trackers as means for improving the performance of photovoltaic generation systems. Two experimental test setups were designed, implemented and used to collect the evaluation results at a site that is located at 28° N latitude, 31° E longitude. One of the test setups included a monocrystalline photovoltaic (PV) panel that is fixed at a reference inclination angle of 28° with respect to the horizon, and facing due south. Whereas, the other experimental setup included an identical photovoltaic panel that is equipped with a solar tracking system, which enables it to continuously follow the sun trajectories. The solar tracking syst em has been designed and developed using a set of light dependent*
resistors (LDR) serving as solar radiation intensity sensors and an Arduino microcontroller (RB-Ard-11) on which the tracking algorithm was programmed. An analytical model to characterize PV cells is presented based on explicit methods, allow the current and the voltage at key operational points, (i.e., in particular at the maximum power point) to be calculated using the single-diode model as a function of cell temperature, irradiance and common manufacturers data. A theoretical analysis has been presented for the modelling of thermal and electrical processes of the solar cell. Energy balance equations have been developed for the various components of the system. Based on the developed analysis, both thermal and electrical performance of the system as a function of system design parameters are presented and discussed. Various performance parameters are calculated for conventional photovoltaic cell for given sets of operating conditions the theoretical and experimental mean photovoltaic cell temperatures can be obtained. Comparisons are made between the experimental and theoretical results under the same operating conditions and close agreement between these two values are obtained. This study showed that the net power produced by the photovoltaic panel increased by about 23.15% and 29% when equipped with single-axis and dual-axis solar tracker, respectively, as compared to the reference case of a fixed mount panel. An analytical model is used to characterize PV cells. The used expressions, based on explicit methods, allow the current and the voltage at key operational points, (i.e., in particular at the maximum power point) to be calculated using the single-diode model as a function of cell temperature, irradiance and common manufacturers data.

Index Terms –DC motor, dual-axis solar tracker, fixed mount solar system, PV cell, and single-axis solar tracker**..**

I. INTRODUCTION

the global energy crisis, along with the call to reduce the ever growing levels of polluting greenhouse gas emissions, inspired the urgent need for increased deployment of renewable energy sources within the electric power system. Among the various renewable energy generation technologies, such as wind, fuel cells, biomass, etc., solar photovoltaic (PV) is the main focus of this paper. PV systems are quite popular and effective, especially in countries where location, climate and topography guarantee high and persistent levels of solar radiation throughout the year. The materials used for PV cell manufacturing limit its efficiency [1]. Monocrystalline Solar Panels have efficiency of approximately 18%. They are made of a large crystal of silicon. This type of solar panels is efficient as in absorbing sunlight and converting it into electricity, however it is relatively expensive. Monocrystalline Solar Panels outperform other types of solar panels in lower light conditions [2],[3].Polycrystalline Solar Panels have efficiency of approximately 15%. Instead of one large crystal, this type of solar panel consists of multiple smaller silicon crystals. They are currently the most commonly used solar panels in the market. They look much like shattered glass. They are slightly less efficient than the Monocrystalline Solar Panels, yet they are less expensive to produce [2], [3]. Amorphous Solar Panels have efficiency of approximately 10%. They consist of a thin-like film made from molten silicon that is spread directly across large plates of stainless steel or similar material. The advantage of the amorphous solar panels over the other two types is that they are shadow protected. That means when a part of the solar panel cells are shaded, the solar panel continues to produce power. This type of solar panels has lower efficiency than the other two types, and is the cheapest to produce [2].The energy produced by PV modules depends not only on their relatively-low efficiency, i.e. typically somewhere around 20%, but also on the alignment of the panels. The sunlight consists of two components; the direct beam, which carries 90% of the solar energy and the diffuse sunlight, which carries the rest of the energy. In order to harness the maximum

International Journal of Academic Engineering Research (IJAER)
ISSN: 2000-001X
Vol. 3 Issue 1, February – 2019, Pages: 1-1

amount of energy, the PV panels should be perpendicular to the direct beam. In other words, they have to be perfectly facing the sun such that the incidence angle is 90°. If the incidence angle is less than 90°, the solar power drops by the cosine of the misalignment angle. The sun travels daily from the east to the west. Therefore, a fixed mount PV panel will be perfectly aligned with the direct beam only during the noon time. However, during early morning and late afternoon times, the misalignment angle of the incident light will lead to reduced utilization of the solar power. Single axis trackers normally use a polar mount for maximum solar efficiency and employ manual elevation (axis tilt) adjustment on a second axis, which can be adjusted regularly during the year[4-5].The system is tracked around a polar N-S axis. The half rim angle of the first concentrating stage is chosen equal to the sun' s maximum declination of 23.5" . So the radiation received by the entrance area of the second stage subtends an angle of 23.5" in both direc- tions. In the nonimaging second stage the solar flux is concentrated further until its divergence. In practice, the ambient temperature, cell temperature and wind speed sometimes play a vital role in drifting the sought-after benefits of solar tracking systems. This work is based on experimental analysis to assess the tradeoff between added complexity and increased productivity of tracker-based PV systems.The main contributions of this paper can be summarized as follows,

- A single-axis/dual-axis microcontroller-based solar tracking system with a low cost will be presented.
- Assessment of the performance of fixed mount PV panels versus single axis and dual axis PV panels will be analyzed through experimental results.

2. METHODOLOGY

Design concept : A typical solar tracking PV system, as shown in Fig. 1, must be equipped with two essential features: (a) Azimuth tracking for adjusting the tilt angle of the surface of the PV panel during changing seasons; and (b) daily solar tracing for maximum solar radiation incidence. The Tilt Angle (θ) of a PV system required at any given time in the year can be expressed as a function of the seɔasonal sun's altitude (ø) as θ =90°- ø [11].

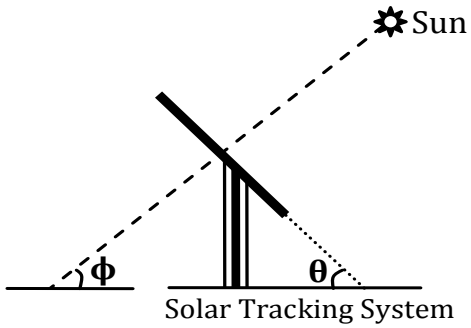

Fig 1: Relation between the tilt angle and the sun's altitude of a PV Array.

System design: Dual axis tracking systems move the solar panel both vertically and horizontally. A schematic block diagram of the proposed solar tracker is shown in Fig. 2. Four

LDR sensors were used to send the feedback signals. Light dependent resistor (LDR) was used to construct the sensor, because of its high reliability. To sense the position of the sun in one axis, say east/west, two LDR sensors were mounted on the solar panel and placed in an enclosure as shown in Fig. 3. It has a response, which is analogous to the human eye. Fig. 3(a) describes the case when the sun's position shifts, and the incidence angle is not maximum. The two LDR sensors, which are located at the right and left hand sides of the panel for single axis tracking, in addition to the two sensors placed on the top and bottom of the panel for dual axis tracking, detect the light source intensity difference. The difference is translated into difference in node voltages sent to the respective Analog to Digital Converter (ADC) channels of the Arduino microcontroller. The Arduino microcontroller calculates the node voltage differences and compares them with the reference set values. Then, it generates the necessary logic signals to actuate the DC motors in such a direction that causes the light intensities on LDRs in each pair to be less than a pre-defined threshold [2], to reach the desired condition depicted in Fig. 3(b).

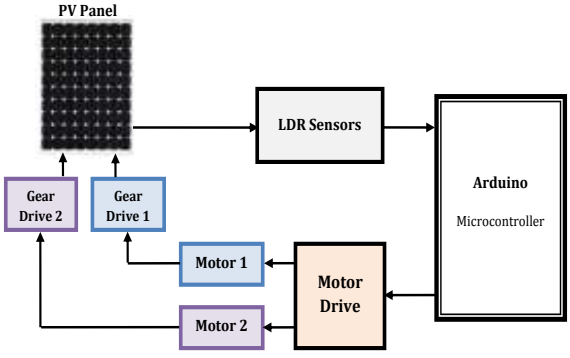

Fig. 2: Block diagram of the solar tracker.

International Journal of Academic Engineering Research (IJAER)
ISSN: 2000-001X
Vol. 3 Issue 1, February – 2019, Pages: 1-1

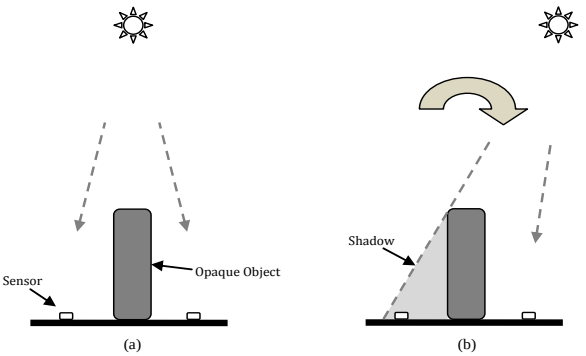

Fig. 3: Illustrates the work of the sensors.

3. EXPERIMENTAL TEST SETUP

A PV system has been constructed at the Department of Mechanical Engineering, Menya University, Menya, Egypt, which is located at 28° latitude, to carry out the experiments. The measurements were collected on a clear day from 9:00 am to 4:00 pm on Sept. 23, 2014 and Oct. 2, 2014, with a sampling rate of 1 hour. The measured data include the solar radiation intensity, ambient temperature, solar cell temperature, wind speed, short circuit current and open circuit voltage.In this work, the fixed mount solar panel was inclined at 28° degree to the horizon, and facing due south.

3.1 Mechanical Construction

The single-axis solar tracking system, consists of a PV panel rotating around a tilted shaft under the action of a bidirectional DC motor controlled according to the real sun position estimated by means of two light intensity sensors. The light sensors consist of two LDRs placed on both sides of the panel, and separated by an opaque plate. Depending on the intensity of the sun rays, one of the two LDRs will be partially shadowed and the other will be illuminated. The LDR present in the side, in which the intensity of the sun rays is higher, will generate a stronger signal and the other will generate a weaker signal. The difference in the output voltage between the two LDRs will drive the movement of the PV panel in the direction in which the intensity of the solar irradiance is maximum. The dual-axis solar tracker follows the angular height position of the sun in the sky in addition to following the sun's east-west movement. The developed dual-axis works in the same way as the single-axis. It consists of two sets of phototransistor sensors and two DC motors. One set of sensors and one motor is used to rotate the cell from the east to the west direction while the other set is used to rotate the tracker from the north to the south direction. The sensor senses the light from the sun and sends the signals generated to the controller. The complete mechanical structure of the proposed single axis and dual axis solar tracker is illustrated in Fig. 4. An Aluminum frame has been used to hold up the weight of the PV panel. LDRs have been placed on the frame of the PV panel. In addition, Fig. 2 shows the position of the two servo motors and the gears that were used to obtain the required torque to move the PV panel. Building a simple and cheap structure was aimed with this mechanical structure.

Fig. 4 shows a detailed view of the PV system and its components. The total costs of the designed and developed solar tracker and its components.

1 → Photovoltaic Monocrystalline Solar Panel, 80 Watt.
2 → Aluminum Sheet.
3 → First DC Motor.
4 → Second DC Motor.
5 → Tracker Base.
6 → Two-Dimensional Mechanism.
7 → Right LDR Circuit.
8 → Bottom LDR Circuit.
9 → Left LDR Circuit.
10 → Top LDR Circuit.

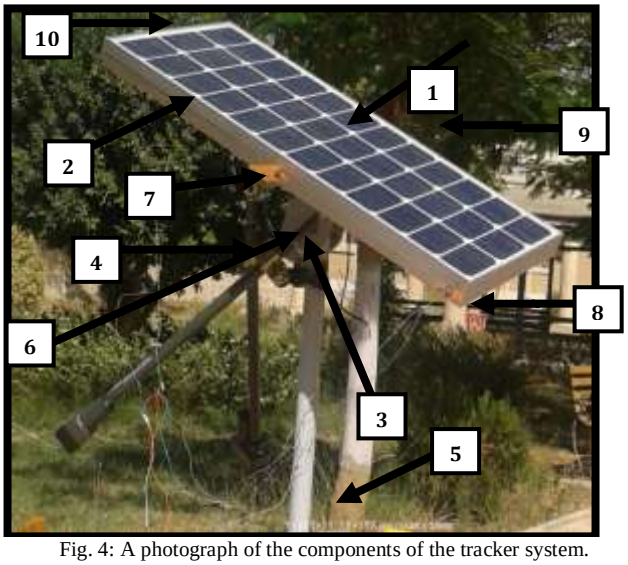

Fig. 4: A photograph of the components of the tracker system.

3.2 Control circuit

The control circuit is powered by a 12V battery, which ischarged by the PV panel itself. Thus, the tracking system does not need any external power supply. The 4 Watt DC motors can turn either in a clockwise or a counter clockwise direction depending upon the sequence of the logic signal sent to the relay circuit motor driver, shown in Fig. 5. Four logic ports of the Arduino microcontroller were used for each channel of the relay circuit motor drive. The sequence of the logic signal depends on the difference of the output from the LDR sensors placed on both sides of the panel. The movement of the two DC motors is decoupled, i.e. the movement of one of the motors is not dependent on the other. Hence, they can move simultaneously when needed.

International Journal of Academic Engineering Research (IJAER)
ISSN: 2000-001X
Vol. 3 Issue 1, February – 2019, Pages: 1-1

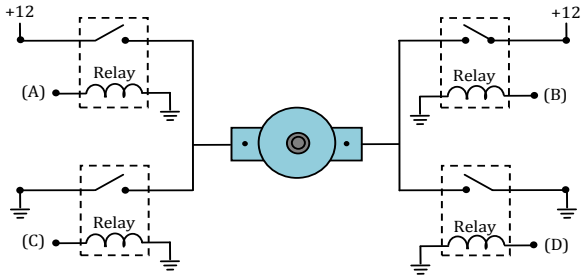

A	B	C	D	Function
1	0	0	1	Forward
0	1	1	0	Backward
1	1	0	0	Brake
0	0	1	1	Brake
1	0	1	0	Fuse test
0	1	0	1	Fuse test

Fig. 5: Relay circuit motor driver.

3.3 Software

Arduino is an open-source electronic microcontroller. The microcontroller is responsible for sending and receiving signals from the robot hardware. The analog readings collected from the sensors placed on the sides of the panel are sent to the Arduino in which they get converted to digital then processed based on the tracking algorithm shown in Fig. 6. In the flow chart of Fig. 7, the collected measurements are namely LDR_1 and LDR_2. A higher reading from any of these two sensors over the other means higher solar radiation at its corresponding side. Assuming that the sensor yielding the signal LDR_1 is placed on the right hand side of the PV panel, while the sensor reading LDR_2 is placed on the left hand side of the panel, see Fig. 3. If the value of LDR_1 is greater than that of LDR_2, the panel should move in an anti-clockwise direction to track the maximum power, and vice versa. In order to avoid steady state oscillations, an acceptable error margin (ε) was enforced, which was set in this case to limit the error in the tracking angle to 1°.

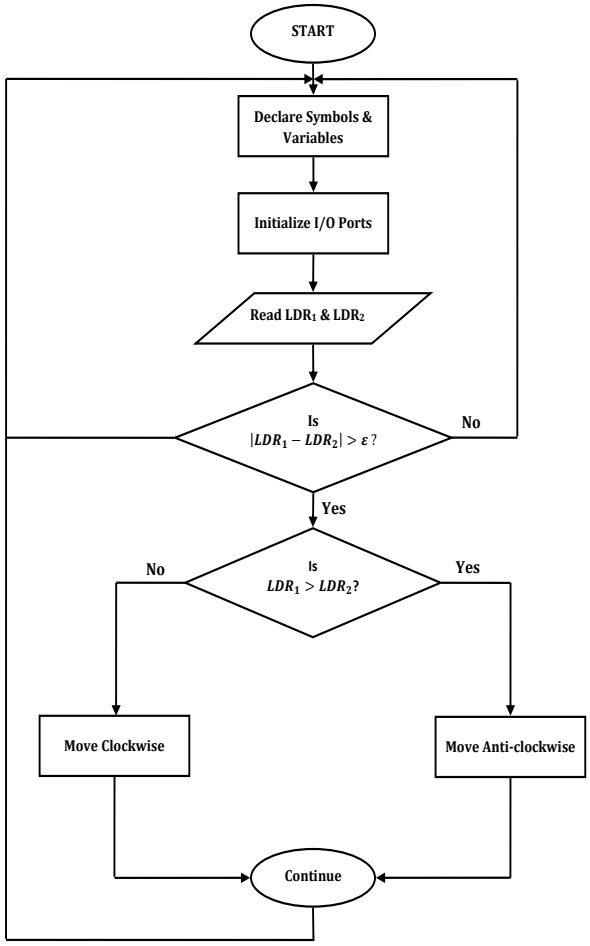

Fig. 6: A flowchart for the implemented tracking algorithm.

3.4 Energy Balance

There has been appreciable works carried out for study of the model performance to different operating condition. All previous is investigation agreed that performance of PV cell respect with increasing temperature [128-131]. In the present work, a simulation model is developed for performance analysis of a conventional photovoltaic cell. Fig 4.27 shows the solar cell with the heat transfer coefficients Square cells 15.4× 9 Cm are pasted over a 118 × 51.6 Cm plate the adhesive used for pasting solar cells is characterized by a high thermal conductive and good electric insulating material. Solar cells are pasted over plate at equal distances in equal number of rows and columns per unit area of the surface. In developing the analytic al model, the following assumptions have been made:

1- Steady state of energy transfer has been achieved
2- Construction is of a plate sheet and cell type
3- There is a negligible temperature drops through plate
4- Dust and dirt on the PV are negligible
5- 5-Solar cell efficiency can be represented by a linear decreasing function of its temperature.

3.4.1 Model I

International Journal of Academic Engineering Research (IJAER)
ISSN: 2000-001X
Vol. 3 Issue 1, February – 2019, Pages: 1-1

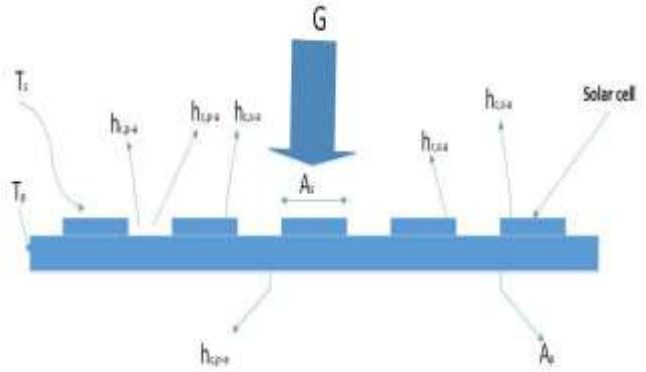

Fig 7 : Schematic of the photovoltaic cell with heat transfer coefficients .

The energy balance equations for various components of photovoltaic cell can be written as follows:

For cell:

$$G * (\tau * \alpha_s) * A_s = h_{sp} * A_s(T_s - T_p) + h_{c,s-a} * A_s(T_s - T_a) + h_{r,s-a} * A_s(T_s - T_a) + E_{(TS)} \quad (1)$$

Where:

$$E_{(TS)} = G * \tau * \alpha_s * A_s * \eta \quad (2)$$

Then,

$$G * \tau * \alpha_s = h_{sp} * (T_s - T_a) + h_{c,s-a}(T_s - T_a) + h_{r,s-a}(T_s - T_a) + G * \tau * \alpha_s * \eta \quad (3)$$

Where:

G : solar radiation

η : the efficiency of the cell

T_s : cell temperature

A : the fraction area of the plate occupied by the solar cells

A_P : is the total panel area

A_s : is the total cell area

h_r, h_c: The convection and radiation hear transfer coefficient from cell and plate to ambient were calculated using the relations given in Duffie and Beckman [131].

For the plate:

$$G * \tau * \alpha_p * (A_p - A_s) + h_{sp} * A_s(T_s - T_p) = h_{c,p-a}(A_p - A_s)(T_p - T_a) + h_{c,p-a}A_p(T_p - T_a) + h_{r,p-a}(A_p - A_s)(T_p - T_a) \quad (4)$$

$$G * \tau * \alpha_p * (1 - A) + h_{sp} * A(T_s - T_p) = h_{c,p-a}(1 - A)(T_p - T_a) + h_{c,p-a}(T_p - T_a) + h_{r,p-a}(1 - A)(T_p - T_a) \quad (5)$$

In which $A = \frac{A_s}{A_p}$

The above equation contains the effect of the solar cells. The solar radiation absorbed by the plate is $(1 - A) * G * \tau * \alpha_p$. Out of the remaining insolation $G * \tau * \alpha_p * A$, which falls on the upper metallic plate, the fraction $G * \tau * \alpha_s * A_S * \eta$ is converted to electrical energy, and the rest $\tau * \alpha_s * A_S * (1 - \eta)$, is transmitted to the plate.

The radiation heat transfer coefficient from the cell to the sky, $h_{r,s-a}$, is :

$$h_{r,s-a} = \epsilon \sigma (T_{sky} + T_s)({T_{sky}}^2 + {T_s}^2) \quad (6)$$

And the radiation heat transfer coefficient from the plate to the sky, $h_{p,s-a}$, is :

$$h_{r,p-a} = \epsilon \sigma (T_{sky} + T_p)({T_{sky}}^2 + {T_p}^2) \quad (7)$$

The convection heat transfer coefficient term, h_c is calculated from the relation

$$h_c = 5.7 + 3.8 * V_w \quad (8)$$

Where V_w is the wind speed (m/s).

The effective temperature of the sky (T_{sky}) is calculated from the following empirical relation [132].

$$T_{sky} = T_a - 6 \quad (9)$$

There must be very good thermal contact between plate and pasted solar cell, there value of the conductive heat transfer coefficient h_{s-p} was taken to equal $150\, W/m^2$℃ .The electrical efficiency of the photovoltaic module has been calculated from the following equation (5.8) [132].

$$\eta = \eta_r[1 - B_r(T_S - T_r)] \quad (10)$$

Where η_r is the cell efficient at the reference temp T_r (25℃) B_r is the temperature correction factor (0.0045/℃) the product of absorptivity and transmissivity was taken to be 0.9.

The procedure is to guess a cell temperature from which $h_{r,s-a}$ and $h_{r,p-a}$ are calculated. With these heat transfer coefficients T_S and T_p are calculated from the above equations. If T_S is close to the initial guess, no further calculations are necessary. Otherwise, the newly calculated T_S is used and the process is repeated.Thermal and

electrical performance of the system as a function of system design parameters are presented and discussed.

5.3 Model II

As found in the literature [133], the cell temperature (Tc) can be calculated using the following well known equation:

$$T_c = T_a + \frac{(NOCT - 20) * S}{800} \qquad (11)$$

The cell temperature is based on the ambient temperature, Ta, solar radiation, S, and the normal operating cell temperature, NOCT.

The NOCT is calculated from the work of Bharti R et al. [134]. The NOCT is function of the ambient Temperature at the sunrise time T_{rise} as follows:

$$NOCT = 20℃ + T_{rise} \qquad (12)$$

It can be calculated from Eq. (12) that the rate of heating of the PV panel, is dependent on the following:

i. The ambient Temperature
ii. The solar radiation
iii. The NOCT

The NOCT has a constant value, while the solar radiation and the ambient Temperature are function of time. Therefore, the cell temperature will be function of time between sunrise and sunset. The solar radiation, the ambient temperature, wind velocity, and the cell temperature were measured between the sunrise and sunset. The cell temperature (Tc) has been calculated using model I and model II and compared to the measured cell temperature. Thermal and electrical performance of the system as a function of system design parameters are presented and discussed

4. Results and discucion

The characteristic behavior of both I–V and P–V characteristic curves obtained by using Salux E. et al [12]. model and the known parameters from the datasheet, Table 4.1 as well as the unknown parameters obtained from MATLAB simulation for the "SU-KAM POWER LT. Model No. FS-M-125and the measured data is plotted in Figs. 7 – 17. The measurements were collected on three different test days to cover two different seasons; Sept. 23, 2014, Oct. 02, 2014, and Feb. 02, 2015.Fig. 7 and Fig. 8 shows I–V and P–V characteristic curves for the tested cell under standard test conditions, STC, i.e., irradiance of 1000 W/m^2, cell temperature of 25 ^{o}C and AM1.5 spectrum, and under Nominal Operating Cell Temperature (NOCT) conditions 45 ^{o}C.The maximum power, maximum current and maximum voltage obtained from the calculations has been compared with the specification data in table 4.1 and a good agreement is achieved.

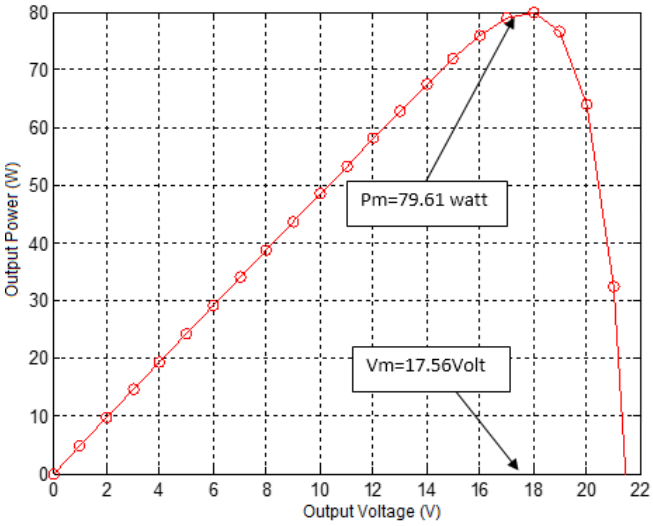

Fig. 8: P-V Curve simulated at Standard Test Conditions.

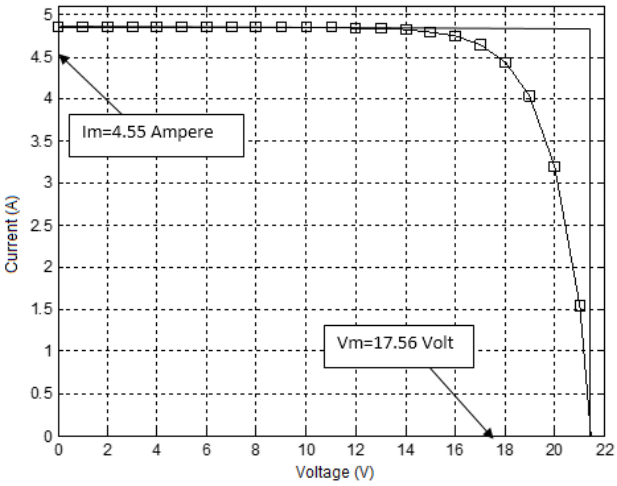

Fig. 9 I-V Curve simulated at Standard Test Conditions.

4.1 *Characterize PV cells under outdoor environment conditions:*

In Practice PV cells do not operate under standard conditions. The two parameters that have the most bearing on their performance are temperature and irradiance.Using the measured data of short circuit current, open circuit voltage, solar radiation, cell temperature, wind velocity and ambient temperature, the following results could be obtained and presented for the tested solar cell.

International Journal of Academic Engineering Research (IJAER)
ISSN: 2000-001X
Vol. 3 Issue 1, February – 2019, Pages: 1-1

4.2 *Efficiency of Single-Axis Tracking System over Fixed Mount*

The power output for the single-axis and fixed mount panel are tabulated for a single day. The average power values prove that the single-axis panel produces more power than that of the fixed mount. The power efficiency calculated for the single-axis solar tracker is said to be 23.15 % more than that of the fixed mount. The tabulated values are simulated and the graph is obtained using MATLAB .Simulation Result for Comparison of Fixed mount and Single-Axis Tracker System are shown in Figs.9 and 10.

Table 1: Specification of the PV moduleMonocrystalline (1000W/m^2, 25 ℃)

Parameters	Values
Max power (Pmax)	80 W
Maximum power voltage (Vm)	17.7 V
Maximum power current (Im)	4.55 A
Open circuit voltage (Voc)	21.4 V
Short circuit current (Isc)	4.85 A
Temperature coefficient of Isc	0.05% /K
Temperature coefficient of Voc	-0.36 %/K
Temperature coefficient of Pmax	-0.45%/K
NOCT	45 ℃
quality factor (N)	1.4
Ideality factor (A)	1.4
Solar Cells	36 cells (118 cm x 51.6 cm) in a 3x12 matrix connected in series
Weight	9 Kg

Table 2: Fixed Vs Single-Axis on test day Sept. 23, 2014.

HOUR	Power for Fixed mount (W)		Net Power for single axis (W)	
	$P_{th}= I_{SC}*V_{OC}$	$P_m=I_m*V_m$	$P_{th}= I_{SC}*V_{OC}$	$P_m=I_m*V_m$
`8.30 am	46	13.9967	53.37	21.7176
9.30 am	62.56	28.8546	68.1326	38.3394
10.30 am	79.91	51.4024	84.155	62.2155
11.30 am	86.107	61.2919	82.78	60.2712
12.30 pm	82.60	58.1212	82.38	61.2769
13.30 pm	82.32	54.1532	81.88	63.8591
14.30 pm	66.99	32.9415	78.196	54.7578
15.30 pm	57.19	22.7413	73.7	48.4071

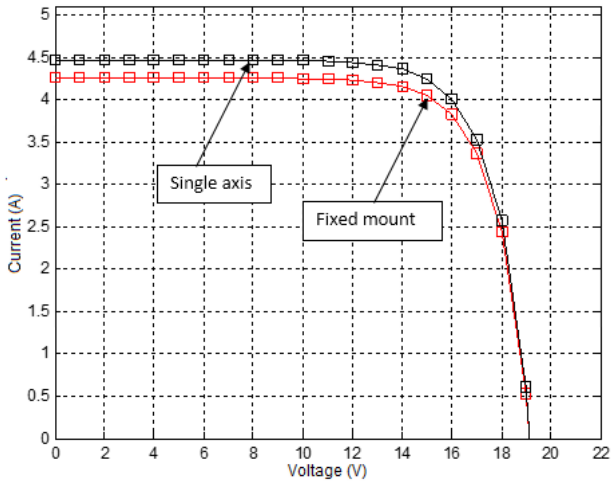

Fig. 10: Comparison of the I-V characteristic for the fixed mount versus the single axis tracker, on test day Sept. 23, 2014.

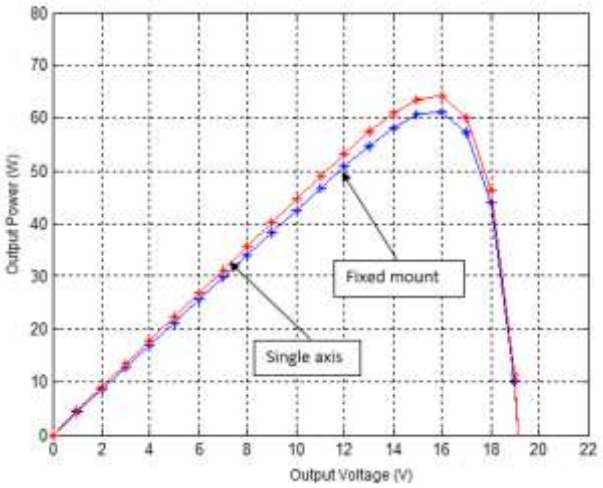

Fig. 11: Comparison of the P-V characteristic for the fixed mount versus the single axis tracker, on test day Sept. 23, 2014.

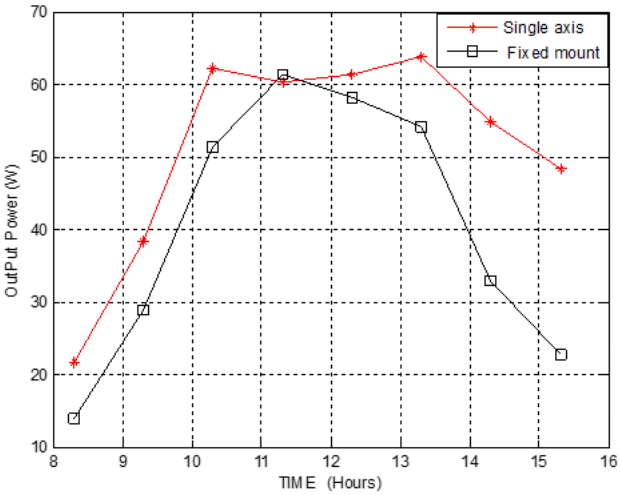

Fig. 12: Simulation Result for Comparison of Fixed mount and Single-Axis Tracker System, on test day Sept. 23, 2014.

International Journal of Academic Engineering Research (IJAER)
ISSN: 2000-001X
Vol. 3 Issue 1, February – 2019, Pages: 1-1

4.3 Efficiency of Dual-Axis Tracking System over Fixed Mount

The power output for the dual-axis and fixed mount panel are tabulated for a single day. The average power values prove that the dual-axis panel produces more power than that of the fixed mount. The power efficiency calculated for the dual-axis solar tracker is said to be 29 % and 31.59% on test days Oct. 02, 2014 and Feb. 02, 2015 respectively more than that of the fixed mount. The tabulated values are simulated and the graph is generated using MATLAB. Simulation Result for Comparison of Fixed mount and dual-Axis Tracker System are shown in Figs.12 and 13.

Table 3: Fixed vs Dual-axis on test day Oct. 02, 2014.

HOUR	Power for Fixed mount (W)		Net Power for dual axis (W)	
	$P_{th}= I_{SC}*V_{OC}$	$P_m=I_m*V_m$	$P_{th}= I_{SC}*V_{OC}$	$P_m=I_m*V_m$
`8.30 am	55.20	18.9232	75.08	42.2476
9.30 am	78.21	44.5495	85.6	57.5007
10.30 am	88.72	59.5655	87.452	60.4204
11.30 am	90.9	63.6858	87.60	61.8130
12.30 pm	86.747	58.9829	82.57	57.1079
13.30 pm	75.3	42.5347	83.336	57.3370
14.30 pm	62.217	27.2271	80.76	52.4934
15.30 pm	48.35	15.5225	77.39	48.3458

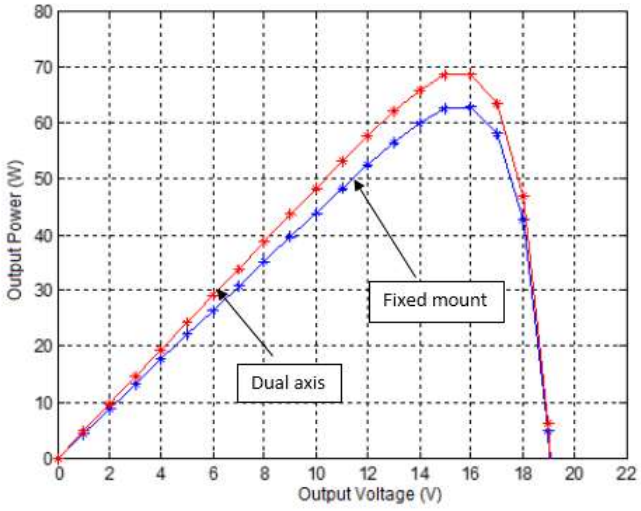

Fig. 13: Simulation Result for Comparison of Fixed mount and Single-Axis Tracker System, on test day Oct. 2, 2014.

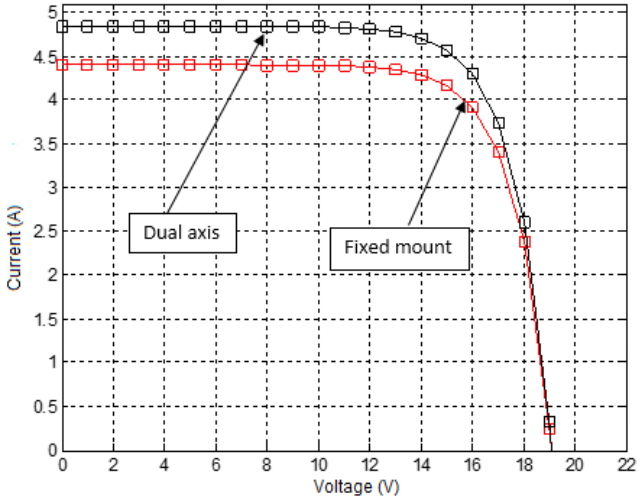

Fig. 14: Comparison of the I-V characteristic for the fixed mount versus the Dual axis tracker, on test day Oct. 2, 2014.

The power output for the dual-axis and fixed mount panel are tabulated for a single day in winter. The average power values prove that the dual-axis panel produces more power than that of the fixed mount. The tabulated values are simulated and the graph is generated using MATLAB. Simulation Result for Comparison of Fixed mount and dual-Axis Tracker System are shown in Figs.15 - 18.The average power values prove that the dual-axis panel produces more power in winter than thatproduces in summer as shown in Figs 17 and Fig. 18. Solar panels work best in certain weather conditions, but since the weather is always changing and as engineers are installing solar panels all over the world in different climate regions, most panels do not operating under ideal conditions. That is why it is important for engineers to understand how panels react to different weather conditions. With this knowledge, they can design ways to improve the efficiency of solar panels that operate in non-optimal conditions. In some cases, they design cooling systems to keep the panels within certain temperatures.

Table 4: Fixed Vs Dual-Axis on test day Feb. 02, 2015.

HOUR	Power for Fixed mount (W)		Net Power for dual axis (W)	
	$P_{th}= I_{SC}*V_{OC}$	$P_m=I_m*V_m$	$P_{th}= I_{SC}*V_{OC}$	$P_m=I_m*V_m$
`9 am	50.89	19.1031	82	46.8403
10 am	65.5	32.9762	84.7	49.7902
11 am	82.69	55.0022	91.275	58.3146
12 pm	88.5	57.4469	89.512	60.8200
13 pm	84.5	50.2071	85.5	54.3447
14 pm	75.8	45.4808	83.45	50.4176
15 pm	66.78	34.8981	81.4	48.2801

International Journal of Academic Engineering Research (IJAER)
ISSN: 2000-001X
Vol. 3 Issue 1, February – 2019, Pages: 1-1

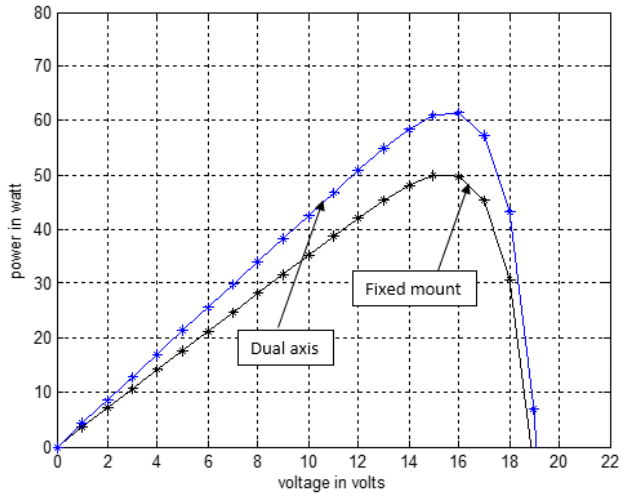

Fig. 15: Simulation Result for the fixed mount versus the Dual axis tracker, on test day Feb. 2, 2015.

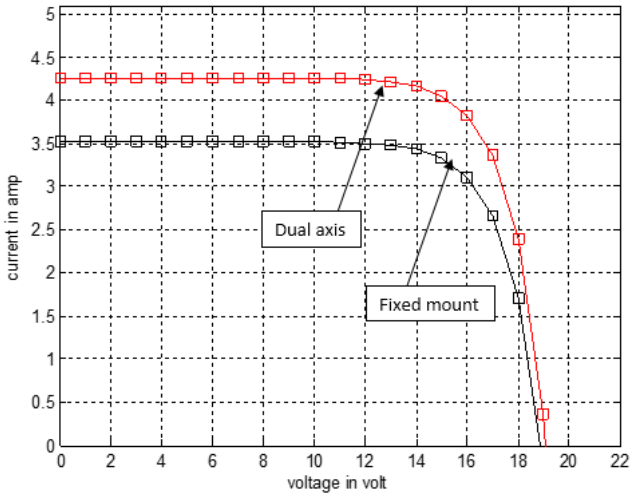

Fig. 16: Comparison Simulation Result for the fixed mount versus the Dual axis tracker, on test day Feb. 2, 2015.

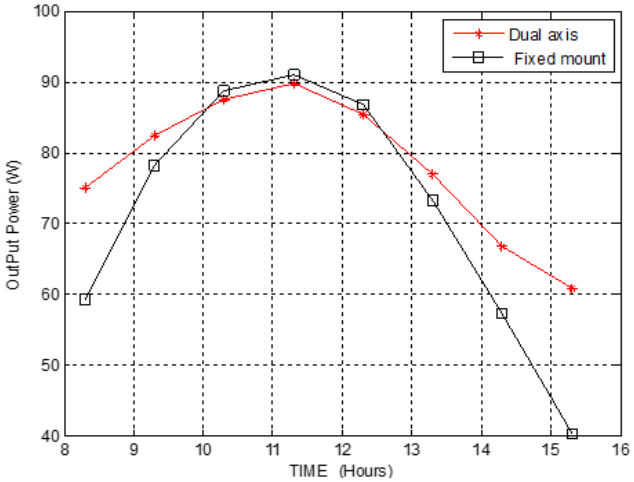

Fig. 17: Simulation Result for Comparison of Fixed Mount and Dual Axis Tracker System, on test day Oct. 02, 2014.

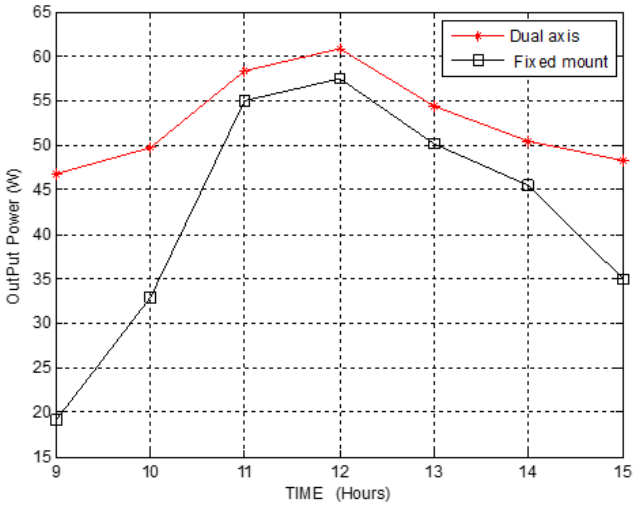

Fig. 18: Simulation Result for Comparison of Fixed Mount and Dual Axis Tracker System, on test day Feb. 02, 2014.

Fig. 19 shows the hourly variation of the solar radiation intensity and short circuit current, for the fixed mount PV panel versus a PV panel that is driven by a single axis solar tracking system on Sept. 23, 2014. Whereas, Fig. 20 shows the variation of the same parameters, for the fixed mount PV panel versus a PV panel that is driven by a dual axis solar tracking system on Oct. 02, 2014. From Figs. 19 and 20, it was observed that both the single and dual axis solar tracking systems lead to higher solar radiation intensity and short circuit current as compared to the fixed mount case throughout the day, on both test days. Figs. 18 and 19 also show that the increase in solar radiation intensity, or in other words, the improvement, decreases as we approach the noon time, specifically between 11:00 am to 13:00 pm in our case. However, the improvement is more significant at the early mornings and late afternoons.

Solar irradiance is a measure of the sun's energy, under standard conditions the amount of energy reaching the Earth's surface on a clear day is taken to be $1kW/m^2$. The amount of irradiance reduces with the slightest amount of haze and becomes quite small on over cast days. I_{SC} is directly proportional to the irradiance: so that if irradiance halves so does I_{SC}. The voltage variation is very small and usually ignored.

International Journal of Academic Engineering Research (IJAER)
ISSN: 2000-001X
Vol. 3 Issue 1, February – 2019, Pages: 1-1

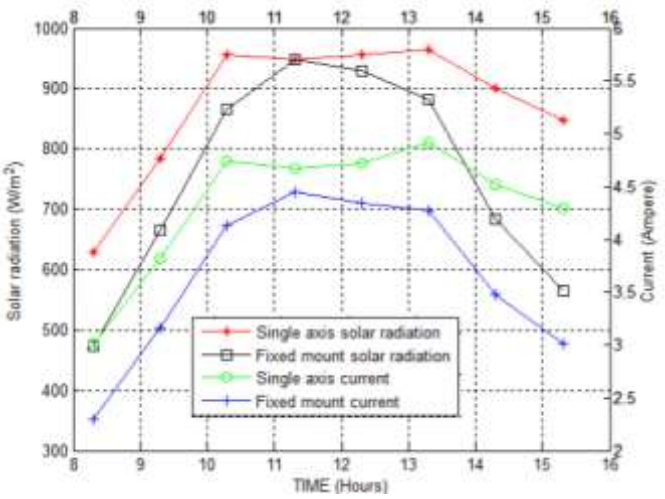

Fig. 19: Variation of solar radiation intensity and short circuit current for fixed mount versus single-axis tracking PV Panel, on test day Sept. 23, 2014.

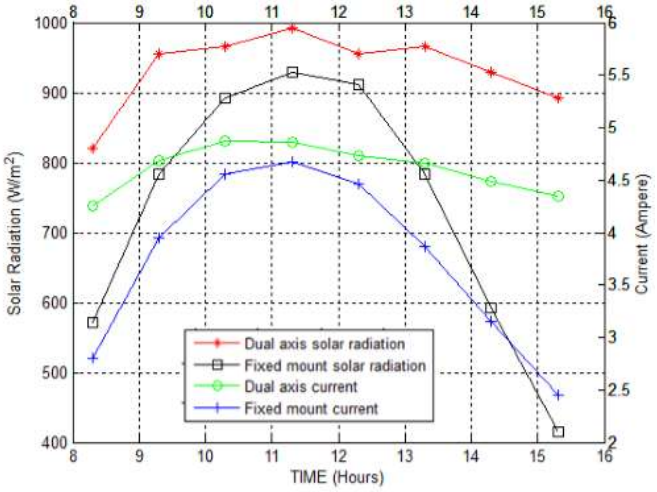

Fig. 20: Variation of solar radiation intensity and short circuit current for fixed mount versus single-axis tracking PV panel, on test day Oct. 02, 2014

The hourly variations of the cell temperature and cell efficiency are shown in Figs. 21 and 22, for the single axis on test day Sept. 23, 2014 and the dual axis on test day Oct. 02, 2014, respectively. These figures show that the increase in cell temperature decreases the cell efficiency in all cases. Figs. 21 and 22 also show that the single axis tracker and dual axis tracker generally increase the efficiency of a PV panel as compared with the fixed mount case.

However, it is worth mentioning that in some intervals, when the ambient temperature is too high, the dual axis tracking system may practically slightly deteriorate the efficiency of the panel. This can be noticed between hours 10:15 am and 12:30 pm in Fig. 21. This problem can be overcome if proper cooling is utilized, subject to the techno-economic feasibility of such a solution, which justifies the need for detailed thermal analysis for solar-tracker-based PV panels.

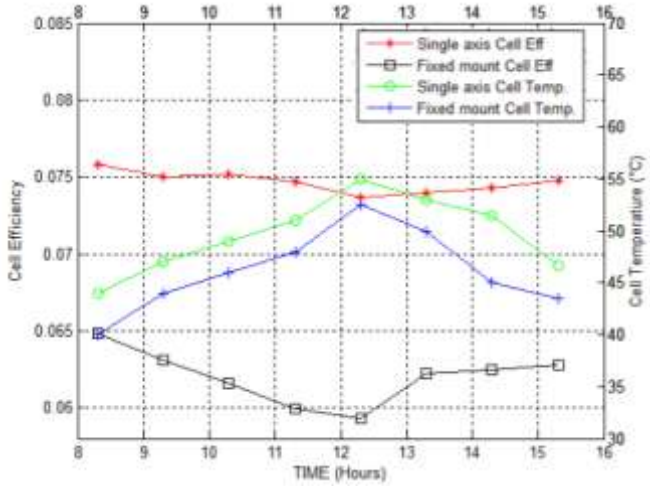

Fig. 21: Comparison of the net efficiency for the fixed mount versus single axis solar tracker panel, on test day Sept. 23, 2014

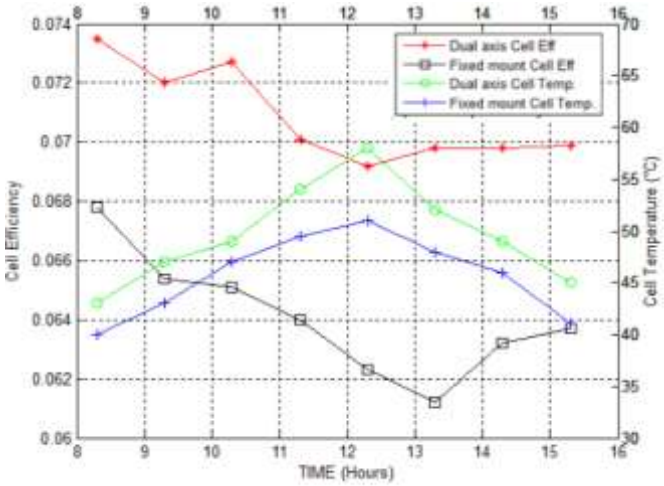

Fig. 22: Comparison of the net efficiency for the fixed mount versus dual axis solar tracker panel, on test day Oct. 02, 2014.

Dual axis tracking systems increase the productivity of solar systems, taking into account seasonal variations. Fig. 23 shows the hourly variation of the solar radiation intensity and short circuit current, for the fixed mount PV panel versus a PV panel that is driven by dual axis solar tracking system at a different season, on a relatively cold test day, Feb. 02, 2015. From Figs. 24 and 25, the dual axis solar tracking systems lead to higher daily average solar radiation intensity and short circuit current of 15.6 % and 15.6 %, respectively, as compared to the fixed mount case.

This is consequently translated into an increase in the resulting output power as shown in Fig. 23. It can also be concluded from Fig. 23 that the problem of high ambient temperature around the noon time, which resulted in

International Journal of Academic Engineering Research (IJAER)
ISSN: 2000-001X
Vol. 3 Issue 1, February – 2019, Pages: 1-1

decreased output power for about two hours in the hot weather (Sept. and Oct., 2014) is not seen in the cold weather (Feb, 2015). The increased output power is noticed throughout the whole day. The daily average output power increased by 31.6%, which means that dual axis tracking systems perform better in the cold we

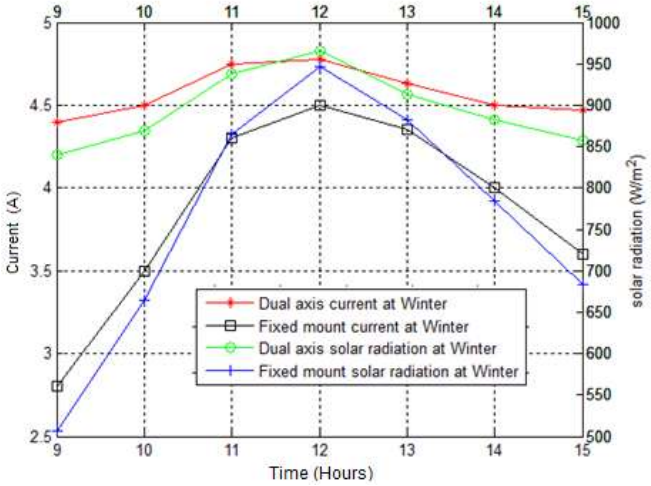

Fig. 23: Variation of solar radiation intensity and short circuit current for fixed mount versus dual-axis tracking PV panel, on test day Feb. 02, 2015

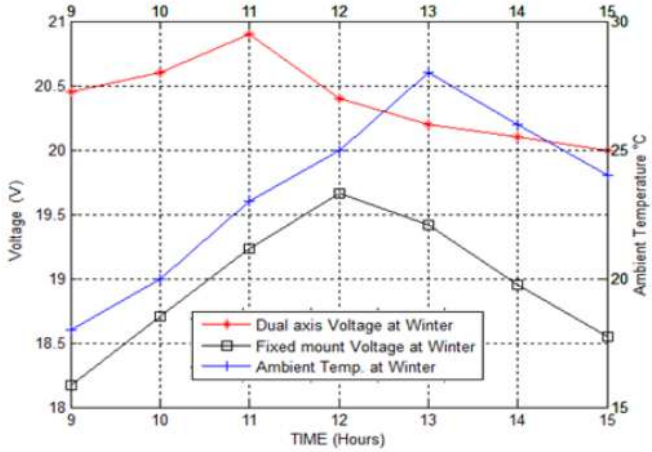

Fig.24: Variation of ambient temperature and open circuit voltage for fixed mount versus dual-axis tracking PV panel, on test day Feb. 02, 2015

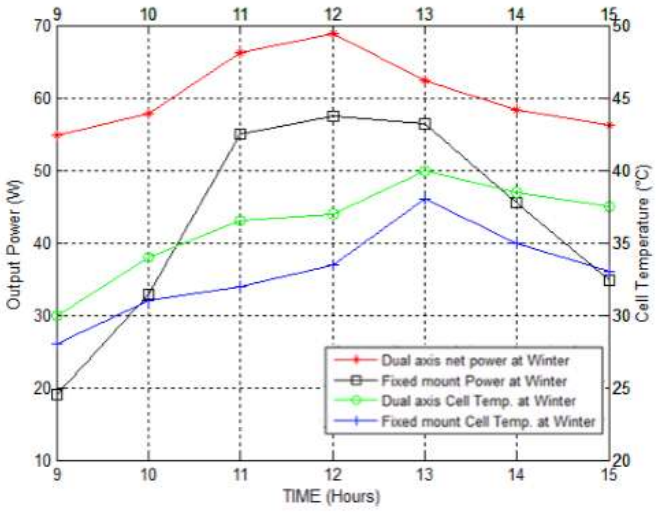

Fig. 25: Comparison of the output power and cell temperature for the fixed mount versus the dual-axis tracker, on test day Feb. 02, 2015

4.4 Numerical Results (Model I)

Results of the simulation are discussed is subsequent figures. Figure.26 present the variation of power and cell temperature as a function of solar intensity. It has been observed that power and solar cell temperature increase with increase in solar radiation intensity keeping in mind that, the remaining operation conditions are kept constant. Ta= 25[℃] , Vw= 1[m/s].

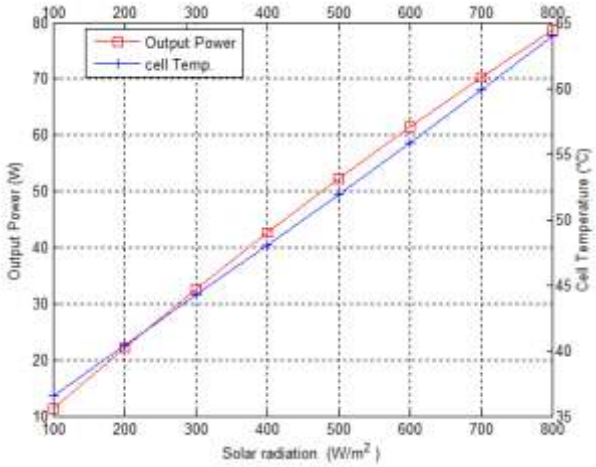

Fig 26. The effect of solar radiation on the power and cell temperature

Figure 27 represents the variation of the PV power and its temperature as a function of the ambient air temperature. The impact of increasing temperature is shown in the figure below. This indicates that increasing ambient air temperature reduces the PV power, however its increase the cell temperature the lower solar cell power for higher ambient air temperature is on account of the higher solar cell temperature. Therefore, the solar cell power is observed to be decreased with increase ambient air temperature is kept constant. In a solar cell, the parameter most affected

International Journal of Academic Engineering Research (IJAER)
ISSN: 2000-001X
Vol. 3 Issue 1, February – 2019, Pages: 1-1

by an increase in temperature is the open-circuit voltage. However, a more significant effect is the temperature dependence of voltage which decreases with increasing temperature.

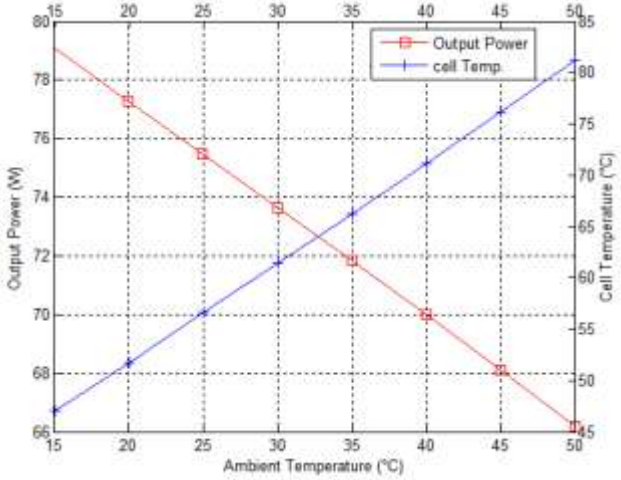

Fig 27. The effect of ambient temperature on the power and cell temperature

The effect of wind speed on the performance of PV is shown in Figure 5.4. It is observed that power has larger value, and the cell temperature has a small value for a larger value of wind speed.

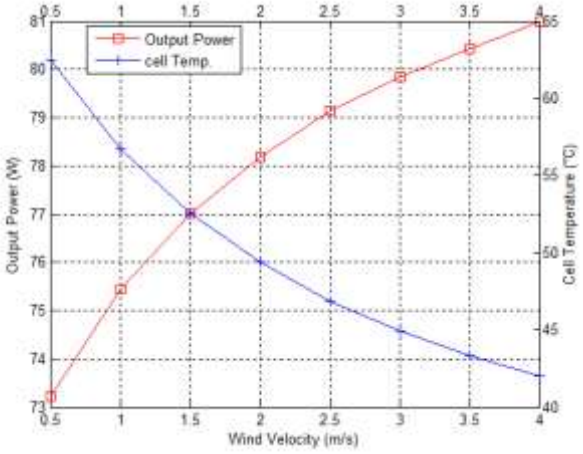

Fig 28. The effect of Wind velocity on the power and cell temperature

The experimental and simulated values of cell, plate temperature and solar cell efficiency during the test day 11-10-2015 are shown in figures 29 and 30 respectively.

Figure 5.6 shows the experimental and simulated values of cell and plate temperatures during the test day 11-10-2014. According to this figure, it is observed that there is a good agreement between the experiments and simulated values of these temperatures.

The experimental and simulated values of cell efficiency during the test day are shown in figure 30. A comparison between the experiment and simulated values of these parameters are carried out in this figure. The cell Temperature (Tc) as calculated by Model 1 and Model 2 and measured is presented in figure 31. The difference between the cell temperatures as measured and calculated does not exceed 0.56. The simulated parameters errors compared with those obtained by the experiment measurements are explained as follows:

Wind speed is not constant and has a direct effect on the heat loses coefficients.

Radiative properties of absorbing surface have been assumed constant while they are changing the day with the change of solar incidence angle on PV surface.

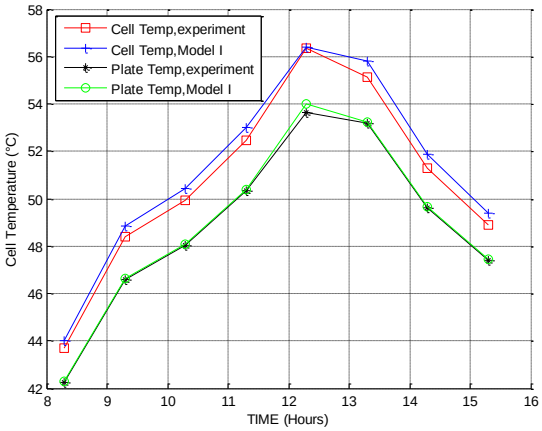

Fig.29: the experimental and simulated values of cell and plate temperature during the test day 11-10-2014

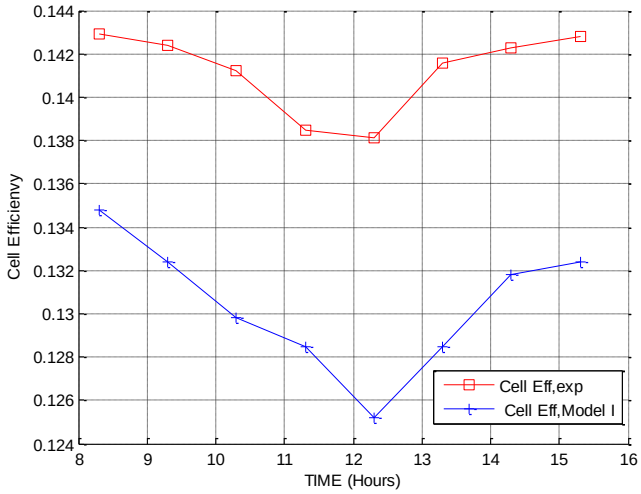

Fig.30: the experimental and simulated values of cell efficiency during the test day 11-10-2014

International Journal of Academic Engineering Research (IJAER)
ISSN: 2000-001X
Vol. 3 Issue 1, February – 2019, Pages: 1-1

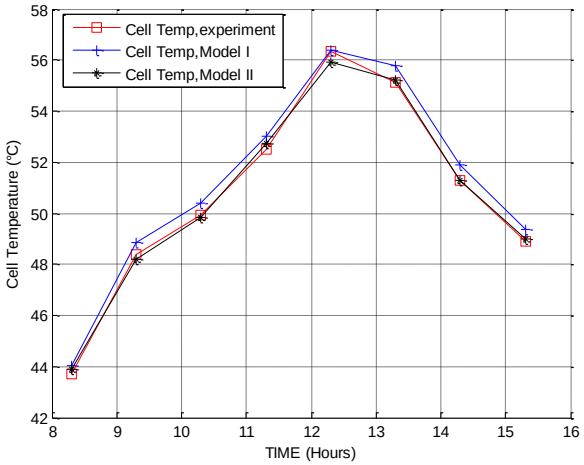

Fig.31: the cell Temperature as calculated and measured during the test day 11-10-2014

5. Conculation

After conducting the experimental and numerical work and discussing the results, few points can be drawn as follows:

1. A microcontroller-based solar tracking system was designed and developed. The logic circuit of the developed tracking system is compact and simple. The results show its effectiveness in improving the performance of PV systems. Based on our experience and market analysis, the developed solar tracking system is simpler and less costly than the other available solar trackers. In summary, the developed solar tracker is simple, cost effective and highly-efficient for trapping the sun's abundant free energy.
2. The net increasing of the average efficiency obtained from the panel with single-axis and dual-axis PV tracking systems are 20.7% and 10 %, respectively compared with the mount fixed on test day Sept. 23, 2014 and Oct. 2, 2014.
3. The daily average solar radiation intensity per unit area of the photovoltaic panel using dual axis solar tracking increased by about 22.5% (Oct. 2, 2014) as compared with that of a fixed mount photovoltaic panel. According to this increase of solar radiation, the daily average of the panel net power, panel temperature, panel short circuit current and maximum current increased by about 29%, 12.6 %, 19.2% and 42% respectively.
4. The daily average solar radiation intensity per unit area of the photovoltaic cell using single axis solar tracking increased by about 13.8% (Sept. 23, 2014) as compared with that of a fixed mount photovoltaic cell. Due to this increase of solar radiation, the daily average of the panel net power, panel temperature, panel short circuit current, and maximum current increased by about 23.14%, 7.5%, 16.8% and 31.4%, respectively.
5. In a hot day, when increasing the solar radiation incidence using solar tracking, the panel efficiency of neither the dual axis solar tracker cell nor the single axis solar tracker improved significantly, as compared with that of the fixed amount cell. This is due to the increase in the photovoltaic panel temperature by about 5.6° C and 3.85° C, respectively.
6. The very high operating temperature of the solar cells approaching noon resulted to a decrease in power generation. Because of that, it is not recommended to use the dual axis solar tracker cell between 10 :00 am to 01:00 pm in the hot weather due to the decrease of the net power compared with that of the fixed mount, unless a cooling method is used, which has to be pre-proved as techno-economically viable.
7. It is preferred to use single axis solar tracking rather than dual axis solar tracking between 10:00 a. m. and 01:00p.m. due to the higher increase of net output power achieved by the single axis as compared with those of the dual axis and fixed mount.
8. The performance of dual axis tracking systems improves in the cold weather. On Feb. 02, 2015, the daily average solar radiation intensity per unit area of the photovoltaic panel using dual axis solar tracking increased by about 15.6% as compared with that of a fixed mount photovoltaic panel. Due to this increase of solar radiation, the daily average of the panel net power , short circuit current and maximum current increased by about 31.6 % ,15.6% and 37% respectively.
9. If the PV left two weeks without cleaning in the experimental place the output power of the cell decreased by about 23% due to dust.

Nomenclature

A	Ideality Factor
DC	Direct Current
I/O	Input / Output
I_m	Maximum Current
I_{sc}	Short Circuit Current
LDR	Light Dependent Resistor
MPP	Maximum Power Point
N	Quality Factor
NOCT	Nominal Operating Cell Temperature
PV	Photovoltaic
P_{max}	Maximum Power
P_{th}	Theratical Power
V_m	Maximum Voltage
V_{oc}	Open Circuit Voltage

Greek symbols

θ	Tilt Angle
ϕ	Sun Altitude

REFERENCES

1- *The Solar Panel How To Guide, Retrieved from http://www.solarpanelsbook.com, Dec. 2010.*
2- *Basil Hamed,* "*Sun and Maximum Power Point Tracking in Solar Array Systems Using Fuzzy Controllers Via FPGA*", *The Islamic University – Gaza, 2011.*
3- *Romy Kansal and Mandeep Singh, PIC Based Automatic Solar Radiation Tracker PATIALA (PUNJAB) -147004, June 2008.*
4- *T. Tudorache et al.:* "*Design of a Solar Tracker System for PV Power*" *Vol. 7, No. 1, 2010.*
5- *Ragunath.G* " *Design and Construction of Micro Controller Based Two Axis Solar Tracking System PHOTO RESISTORS and Real Time Clock*" *Periyar Maniammai University , vallam, Thanjavur (T.N) - 613403, India*
6- *Brunotte M, Goetzberger A, Blieske U.* "*Two-stage concentrator permitting concentration factors up to 300*with one-axis tracking. Solar*" *Energy;56(3):285–300, 1996*
7- *H. Mousazadeh, A. Keyhani, A. Javadi, H. Mobli, K. Abrinia, A. Sharifi* "*A review of principle and sun-tracking methods for maximizing solar systems output* " *Renewable and Sustainable Energy Reviews, Vol. 13, Issue 8, pp. 1800-1818 , 2009.*
8- *R. Sharma, G. Singh, M. Kaur,* "*Development Of FPGA-Based Dual Axis Solar Tracking System,* " *American Transactions on Engineering & Applied Sciences, Vol. 2, Issue 4, pp. 253- 267, 2013.*
9- *Asmarashid Ponniran, Ammar Hashim, and Handy Ali Munir,* "*A Design of Single Axis Sun Tracking System*", *the 5th International Power Engineering and Optimization Conference (PEOCO2011), June 2011.*
10-*A. Ponniran, A. Hashim, A. Joret,* "*A Design Of Low Power Single Axis Solar Tracking System Regardless Of Motor Speed,* " *International Journal of Integrated Engineering, Vol. 3, No. 2, pp. 5-9, 2011*
11-*P.Srinivasarao et al.* " *Design and Development of 10kva Solar Photovoltaic Cells with Fixed and Tilting Panels*" *International Journal of Engineering and Innovative Technology (IJEIT) Volume 2, Issue 1, ISSN: 2277-3754, July 2012.*
12-*Etienne Saloux , Alberto Teyssedou and Mikhail Sorin* " *Explicit model of photovoltaic panels to determine voltagesand currents at the maximum power point* ", *Solar Energy 85 , 713–722, 2011.*